Rational biomarker development for the early and minimally invasive monitoring of AML

Sherif Abdelhamed,[1] John T. Butler,[2,3] Seul Jung,[4] Ding-Wen Chen,[4] Gaye Jenkins,[5,6] Lina Gao,[7] Jeong Y. Lim,[7] Jeffery M. Klco,[1] Terzah M. Horton,[5,6] and Peter Kurre[4,8]

[1]Department of Pathology, St. Jude Children's Research Hospital, Memphis, TN; [2]Department of Pediatrics, Pape Family Pediatric Research Institute, OHSU, Portland, OR; [3]Department of Biomedical Engineering, OHSU, Portland, OR; [4]Children's Hospital of Philadelphia, Comprehensive Bone Marrow Failure Center, Philadelphia, PA; [5]Baylor College of Medicine/Dan L. Duncan Cancer Center; [6]Texas Children's Cancer Center, Houston, TX; [7]Biostatistics Shared Resource, Knight Cancer Institute, OHSU, Portland, OR; and [8]University of Pennsylvania, Perelman School of Medicine, Philadelphia, PA

Key Points

- Candidate discovery of translational feasibility for noninvasive measurement of miRNA from plasma vesicles as a biomarker for AML patients.

- Preclinical validation of miR-1246 (candidate among 15 miRNA) as a potential minimally invasive AML biomarker for early monitoring of MRD.

Recurrent disease remains the principal cause for treatment failure in acute myeloid leukemia (AML) across age groups. Reliable biomarkers of AML relapse risk and disease burden have been problematic, as symptoms appear late and current monitoring relies on invasive and cost-ineffective serial bone marrow (BM) surveillance. In this report, we discover a set of unique microRNA (miRNA) that circulates in AML-derived vesicles in the peripheral blood ahead of the general dissemination of leukemic blasts and symptomatic BM failure. Next-generation sequencing of extracellular vesicle-contained small RNA in 12 AML patients and 12 controls allowed us to identify a panel of differentially incorporated miRNA. Proof-of-concept studies using a murine model and patient-derived xenografts demonstrate the feasibility of developing miR-1246, as a potential minimally invasive AML biomarker.

Introduction

Acute myeloid leukemia (AML) evolves as an aggressive, molecularly heterogeneous disease arising from clonal differentiation arrest and uncontrolled hematopoietic progenitor proliferation in the bone marrow (BM), with late dissemination to the peripheral blood (PB). Early detection of AML has been challenging, with no unifying molecular marker for noninvasive PB-based screening. Rather, symptoms appear late, and disease detection relies on flow cytometry and morphologic assessment of BM aspirates.[1,2] Disease tracking based on cellular assays is further complicated by the prompt clearance of leukemic blasts in circulation during therapy and after remission, when serial BM surveillance is invasive and cost-ineffective.[3,4]

To address the urgent need for an actionable AML biomarker, we considered cell-free microRNA (miRNA) a powerful, minimally invasive metric, and specifically, a subset of circulating AML-associated miRNA that escapes ribonuclease degradation through incorporation into 30- to 130-nm extracellular vesicles (EV^{AML}).[5-8] We hypothesized that plasma EVs from AML patients contain a unique complement of miRNA, whereby EV^{AML} seed the PB ahead of the general dissemination of leukemic cells. Small-RNA sequencing in 12 AML patients and 12 controls allowed us to identify a panel of differentially incorporated miRNA. In a murine model of AML and patient-derived xenografts (PDX), we show that circulating EV^{AML} precede AML blasts and correlate with disease burden, and we validate miR-1246 as a potential noninvasive EV^{AML} miRNA biomarker.

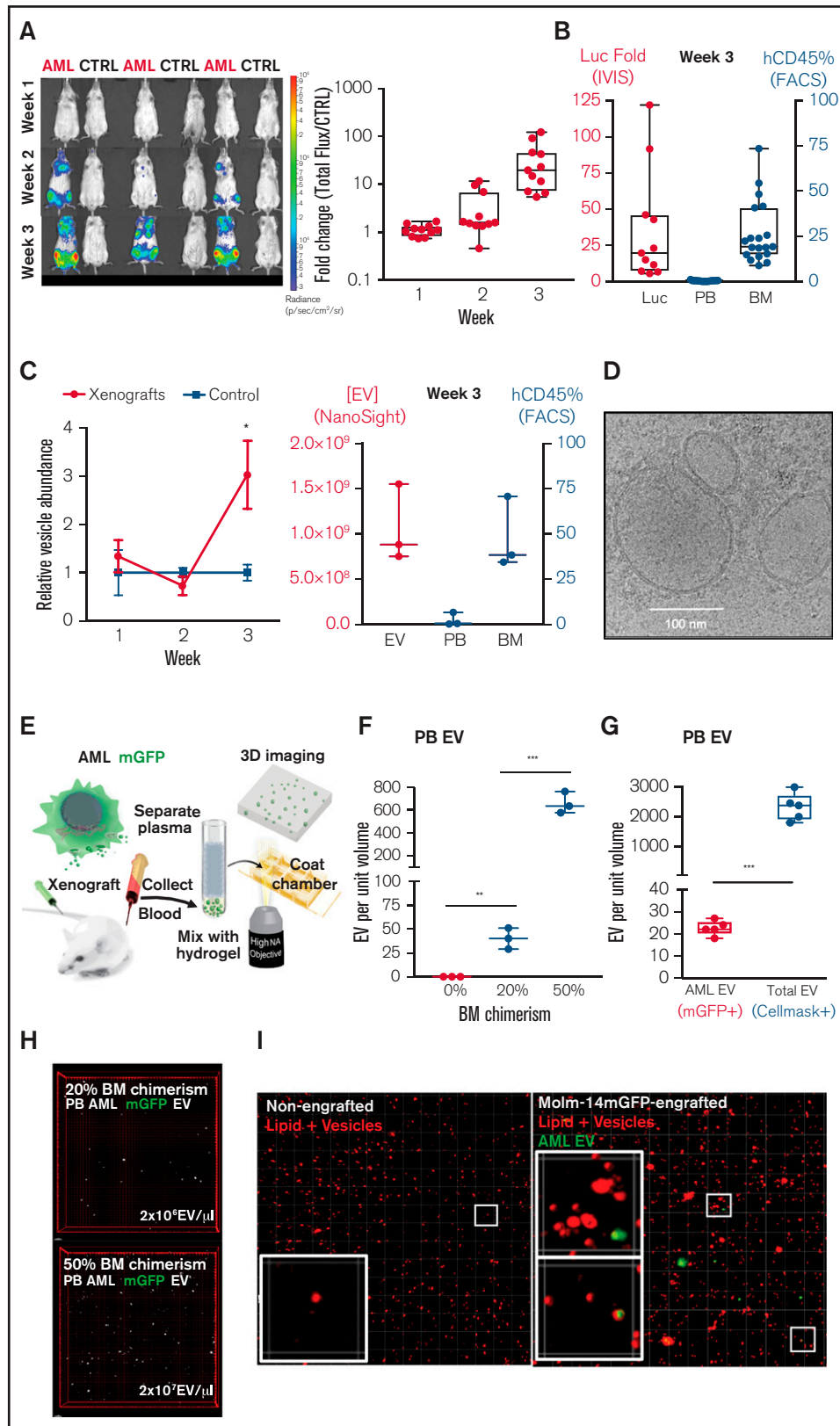The full-text version of this article contains a data supplement.

Figure 1. Correlation between EVs levels and AML disease burden. (A) In vivo imaging of mice xenografted with Molm-14 cells expressing luciferase at 1, 2, and 3 weeks. Images were taken by *IVIS* (left), and values were normalized to controls to calculate fold change (right). (B) Correlative analysis of tumor burden between human CD45 (hCD45) levels measured by flow cytometer in both the PB and BM in red vs luciferase activity in gray. (C) EV quantification using NanoSight analyzer from Molm-14

Methods

Animals

Animal studies were approved by the OHSU and St. Jude's Institutional Animal Care and Use Committee. For Molm-14 xenografts, cells (0.1×10^6 per animal) were transplanted into NOD.Cg-Prkdc^{scid}Il2rg^{tm1Wjl}/SzJ (NSG) mice[7] and imaged by IVIS.[6] For PDX, CD3-depleted blasts were injected into sublethally irradiated NSG-SMG3.

Cells and patient materials

Molm-14 cells were cultured in RPMI 1640 with 10% Fetal Bovine Serum (FBS) and $1\times$ penicillin/streptomycin (ThermoFisher) at 37°C, 5% CO_2. Patient materials were obtained under Institutional Review Board–approved protocols at Texas Children's Cancer Center or St. Jude's Children's Research Hospital.

Flow cytometry

Data were acquired using LSR-FORTESSAII (BD-Biosciences) and analyzed using FlowJo (TreeStar).

Statistics

Student t test was used to assess significance.

Results and discussion

Circulating EV^{AML} concentration correlates with BM disease burden

To formally demonstrate EV equilibration of AML blasts from BM to PB, we modeled AML tumor burden in vivo using our validated Molm-14 xenografts. In vivo imaging of mice bearing Molm-14 cells transduced with luciferase or myristoylated/membrane-targeted Green Fluorescent Protein (mGFP) lentivectors showed a gradual gain in signal (Figure 1A). Luciferase activity matched high tumor burden in the BM measured by human CD45% (hCD45), whereas PB hCD45% was negligible, indicating the characteristic lack of correlation that complicates disease monitoring (Figure 1B). Although we did not detect circulating leukemia cells, we observed a higher overall concentration of circulating EVs in xenografted mice (Figure 1C). EVs are nanoscale particles (Figure 1D) constitutively released by all cell types, but AML EVs (EV^{AML}) are unique in their composition and contribute to disease progression.[6,7] Because we previously showed that AML cells expressing mGFP release EVs that are detectable by microscopy,[7] we determined EV^{AML} concentration in plasma from xenografts and control animals with a 3-dimensional hydrogel-embedding technique for detection of EVs by high-resolution microscopy (Figure 1E). Plasma from mice with ~20% BM chimerism contained ~40 mGFP$^+$ EVs per 1×10^{-4} μL, whereas those with ~50% chimerism had ~658 mGFP$^+$ EVs

per 1×10^{-4} μL, indicating a correlation between circulating EV^{AML} and AML BM burden (Figure 1F,H). EV^{AML} could be distinguished from circulating host EVs by labeling plasma-derived EVs with CellMask a lipophilic dye. Our data demonstrated EV^{AML} (colabeled with CellMask/GFP) make up a sizable fraction of circulating EV, consistent with equilibration between BM and PB and their potential utility as a cell-free biomarker (Figure 1G,I).

Identification of an AML signature from plasma EV miRNA

We recently reported the selective in vitro and in vivo enrichment of miRNAs in EV^{AML5,6}. To identify an miRNA signature specific to AML patients, we performed small-RNA sequencing of EVs, purified from 1 mL plasma by serial ultracentrifugation, of 12 newly diagnosed AML patients (supplemental Table 1) and 12 healthy controls (Figure 2A). NGS-miRNA libraries were constructed using NEB-NEXT kit, and samples were sequenced using the Illumina Next-Seq500. Gene-wise linear models were employed to compare differential expression (DE) in these groups using R/Bioconductor software, limma,[9] and False Discovery Rate (FDR) adjustments.[10] DE genes were defined as greater than or equal to twofold change and FDR ($P < .05$), and 243 miRNAs met criteria (107 upregulated and 136 downregulated in the AML group; Figure 2B; supplemental Figure 1A). Principal Component Analysis (PCA) showed a good separation between the groups using the selected DE miRNAs, supporting the feasibility of a prediction model for AML (supplemental Figure 1B). We identified 15 large-effect size DE miRNAs that were greater than or equal to eightfold upregulated in the AML group with FDR ($P < .05$), including miR−144−5p , miR−96−5p, miR−145−5p, miR−378a−5p, miR−222−5p, miR−181a−3p, miR−181b−5p, miR−199b−5p, miR−3154, miR−92a−1−5p, miR−25−5p, miR−27a−5p, miR−1246, miR−6503−3p, and miR−6503−5p (Figure 2C).

Validating EV^{AML} miRNA in preclinical models

To demonstrate reproducibility and validity, we systematically determined levels of EV^{AML}-associated miR-1246 in plasma from AML xenograft models as a representative miRNA because it was consistent with our previous report of EV^{AML} miRNA from AML cell lines,[5] which exposed it as a high-confidence reproducible candidate independent of the analysis (Figure 2D). We observed a high correlation between miR-1246 levels and tumor burden (hCD45%) in Molm-14 xenografts at week 4, whereas the frequency of PB blasts was negligible (Figure 2E). We further validated our data using 3 PDX models with variable latency (Figure 2F). In the more aggressive model, PDX5, miR-1246 levels were significantly correlated with disease progression (Figure 2G-H). Interestingly, in the long-latency PDX models (PDX1 and 2), miR-1246 levels accurately mirrored the tumor progression at early disease stages despite the low PB

Figure 1 (continued) xenografted (red) or control (black) mice. Data show relative vesicles abundance over time (left) and correlation analysis at week 3 of PB and BM (red) vs EV abundance (blue). (D) Cryo-TEM image of Molm-14–derived EVs. Scale bar is 100 nm. (E) Workflow for measuring circulating EVs in the PB of mice bearing mGFP$^+$ AML cells. (F) EV counts per unit volume (1×10^{-4} μL) correspond to BM tumor burden. (G) Quantification of relative AML EV count in the PB compared with total lipid vesicles in plasma. Each point represents EV count per unit volume (1×10^{-4} μL). (H) Representative 3-dimensional images and concentration of 20% (top) and 50% (bottom) animal cohorts. Bounding box represents 100 μm × 100 μm × 10 μm volume. Concentrations determined using [EVs/μL = (average EV count) × (volume/1) × (dilution factor)]. mGFP (white). (I) PB plasma of AML xenografted NSG mice contain numerous lipid vesicles and a discrete mGFP EV population (right) not seen in nonengrafted control animals (left). CellMask Lipid Dye (red), mGFP (green). Bounding box is 5 μm x 5 μm. Images captured with CoreDV epifluorescence microscope with 100× 1.49 TIRF objective and Nikon Coolpix CCD camera. Significance determined by Student t test. *$P < .05$; ***$P < .001$.
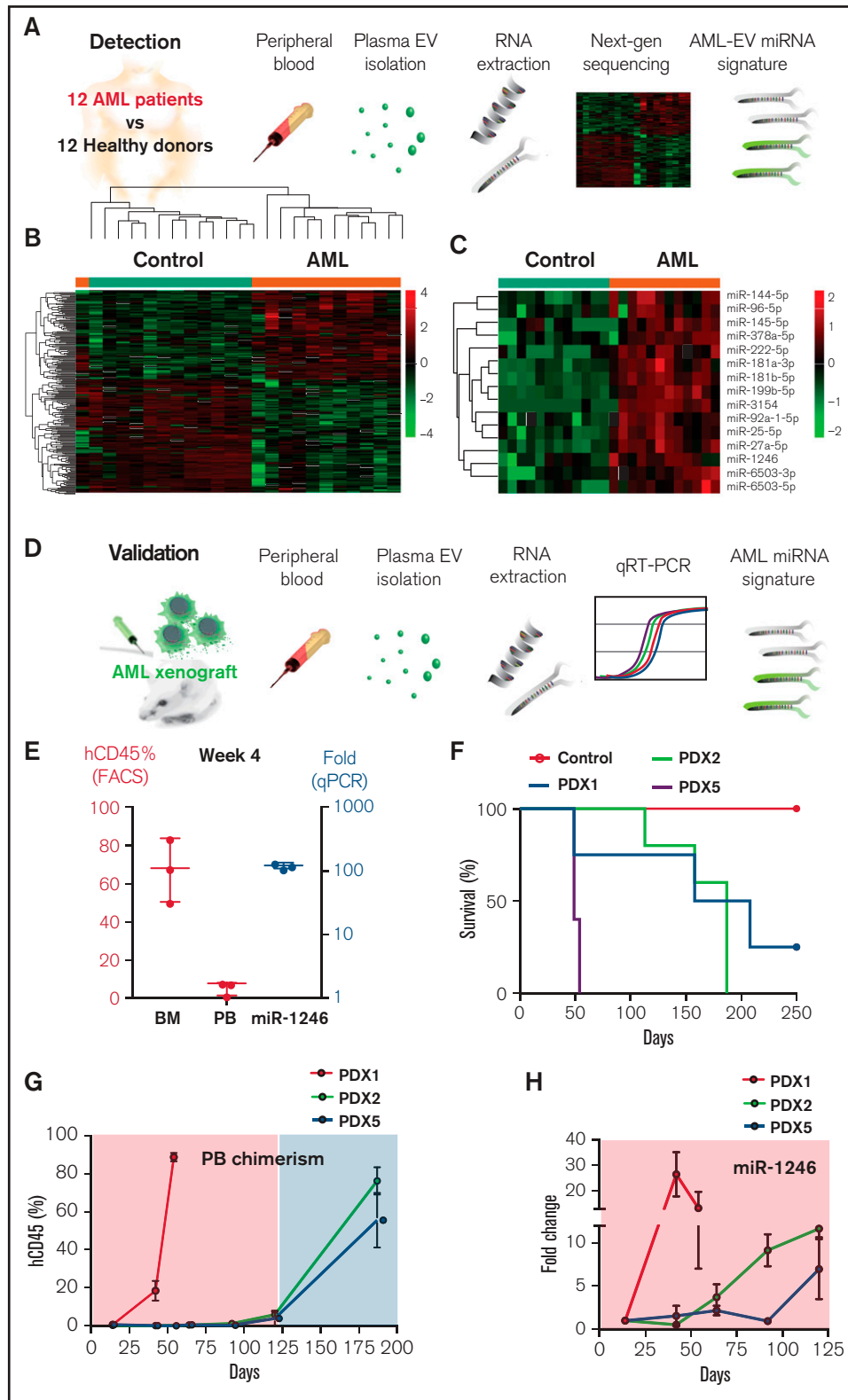
Figure 2. Identification of AML miRNA signature from patients' plasma EVs . (A) Workflow for characterization of EVs miRNA content. The RNA content of EVs from blood plasma collected from 12 AML patients and 12 healthy donors were sequenced using Nextseq500 analyzer. (B) Heat map showing the 243 differentially expressed miRNA between the AML patients (orange) and the healthy donors (green) groups. (C) Heat map showing the AML signature composed of 15 miRNAs uniquely upregulated in the AML patients (orange) vs the healthy donors (green). (D) Workflow for validation of miR-1246, a candidate miRNA among the AML signature. Molm-14 cells or PDXs were executed, and miR-1246 levels were measured in the blood plasma EVs by quantitative polymerase chain reaction (qPCR). (E) Correlative analysis at 4

chimerism (Figure 2G-H). Moreover, miR-1246 monitored residual disease early after chemotherapy initiation, and its levels were higher in patients with elevated blast counts (supplemental Figure 2). Our data, in sum, support further development of plasma EV-miRNA as a minimally invasive biomarker and for longitudinal tracking in AML patients.

Several recent reports support the potential of plasma miRNA as minimally invasive markers of disease.[11,12] However, unlike previous attempts that examined freely circulating miRNAs, we set out to take advantage of the disease-specific enrichment and extended half-life of small-RNAs protected within circulating EVs.[12] An additional advantage, given the molecular and cytogenetic heterogeneity of AML, is that several distinct subtypes appear to share the overexpression of select miRNAs.[13-15] Here, we leveraged these potential advantages for EV^AML and investigated circulating plasma EVs miRNA from a cohort of 12 AML patients vs 12 healthy donors. That screen not only identified a panel of 15 EV-contained miRNAs that distinguish AML patients from healthy controls, but we selectively validated EV^AML miRNA using PDX models from human AML patients. Our data consistently identified miR-1246 as a highly sensitive marker of leukemic burden along with 7 uniformly expressed miRNA as potential normalization controls: let−7i−5p, miR−942−5p, miR−374b−3p, miR−361−3p, miR−589−5p, miR−3613−5p, and miR−885−5p. As previous studies,[13,14] our EV^AML miRNA panel included freely circulating miR−181a−3p, miR−181b−5p, hsa−miR−199b−5p, and miR−6503−3p, suggesting the reproducibility and sensitivity of our analysis, whereas miR-1246 was EV-specific.

Current cell-based markers can provide useful prognostic guidance, but BM-based qPCR and flow cytometry require an invasive and costly aspiration procedure.[1,2] Specifically, our results provide proof-of-principle for miR-1246 (among 15 miRNA) as a potential biomarker for AML for future monitoring of residual disease and early detection of relapse. Follow-up studies will have to test AML subtype specificity and longitudinal performance in patients, ideally pairing EV^AML miRNA(s) with an additional cell-free marker of disease. The generated results serve as preclinical validation and demonstrate the translational feasibility of measuring miRNAs noninvasively from patients' plasma.

Authorship

Contribution: All the authors have approved their authorship in this work, gave input to the manuscript, and contributed as follows: S.A. and P.K. conceptualized the work; S.A., J.T.B., J.M.K., and P.K. provided the methodology; S.A., J.T.B., D.-W.C., and S.J. did the investigating; S.A., J.T.B., L.G., and J.Y.L. provided the formal analysis; S.A. and P.K. wrote the original draft; S.A. and J.T.B. provided the visualization; S.A., G.J., J.M.K., T.M.H., and P.K. provided resources; S.A., J.T.B., and P.K. acquired funding; and S.A., J.M.K., and P.K. supervised.

Conflict-of-interest disclosure: The authors declare no competing financial interests.

ORCID profiles: S.A., 0000-0002-3319-2403; J.T.B., 0000-0001-9945-9791; S.J., 0000-0003-4443-5893; D.-W.C., 0000-0003-2806-0307; L.G., 0000-0001-9382-0419.

Correspondence: Sherif Abdelhamed, St. Jude Children's Research Hospital, Memphis, TN 38105; e-mail: Sherif.Abdelhamed@stjude.org; and Peter Kurre, Children's Hospital of Philadelphia, University of Pennsylvania, Philadelphia, PA 19104; e-mail: kurrep@e-mail.chop.edu.

References

1. Loken MR, Alonzo TA, Pardo L, et al. Residual disease detected by multidimensional flow cytometry signifies high relapse risk in patients with de novo acute myeloid leukemia: a report from Children's Oncology Group. *Blood.* 2012;120(8):1581-1588.

2. Yin JA, O'Brien MA, Hills RK, Daly SB, Wheatley K, Burnett AK. Minimal residual disease monitoring by quantitative RT-PCR in core binding factor AML allows risk stratification and predicts relapse: results of the United Kingdom MRC AML-15 trial. *Blood.* 2012;120(14):2826-2835.

3. Döhner H, Estey EH, Amadori S, et al; European LeukemiaNet. Diagnosis and management of acute myeloid leukemia in adults: recommendations from an international expert panel, on behalf of the European LeukemiaNet. *Blood.* 2010;115(3):453-474.

Figure 2 (continued) weeks in Molm-14 xenografted mice between human CD45 levels measured by flow cytometer in both the PB and BM (red), and miR-1246 levels measured by qPCR and normalized to U6 control (blue). (F) Survival curve of PDXs (n = 5 per group; PDX1, PDX2, and PDX5). (G) Flow cytometer analysis showing PB chimerism represented by hCD45 levels over time in mice (n = 5 per group) xenografted with PDX1, PDX2, and PDX5. (H) qPCR analysis showing fold change of miR-1246 over time in PDX1 (red), PDX2 (blue), and PDX5 (green) relative to week 2. Data were normalized to U6 control (dCT), and fold change was determined relative to nonengrafted controls (ddCT).

4. Hageman IM, Peek AM, de Haas V, Damen-Korbijn CM, Kaspers GJ. Value of routine bone marrow examination in pediatric acute myeloid leukemia (AML): a study of the Dutch Childhood Oncology Group (DCOG). *Pediatr Blood Cancer.* 2012;59(7):1239-1244.

5. Hornick NI, Huan J, Doron B, et al. Serum exosome microRNA as a minimally-invasive early biomarker of AML. *Sci Rep.* 2015;5(1):11295.

6. Hornick NI, Doron B, Abdelhamed S, et al. AML suppresses hematopoiesis by releasing exosomes that contain microRNAs targeting c-MYB. *Sci Signal.* 2016;9(444):ra88.

7. Abdelhamed S, Butler JT, Doron B, et al. Extracellular vesicles impose quiescence on residual hematopoietic stem cells in the leukemic niche. *EMBO Rep.* 2019;20(7):e47546.

8. Caivano A, Del Vecchio L, Musto P. Do we need to distinguish exosomes from microvesicles in hematological malignancies? *Leukemia.* 2017; 31(9):2009-2010.

9. Ritchie ME, Phipson B, Wu D, et al. limma powers differential expression analyses for RNA-sequencing and microarray studies. *Nucleic Acids Res.* 2015;43(7):e47.

10. Benjamini Y, Hochberg Y. Controlling the false discovery rate: a practical and powerful approach to multiple testing. *J R Stat Soc B.* 1995;57(1): 289-300.

11. Mitchell PS, Parkin RK, Kroh EM, et al. Circulating microRNAs as stable blood-based markers for cancer detection. *Proc Natl Acad Sci USA.* 2008;105(30):10513-10518.

12. Abdelhamed S, Kurre P. Hope and hype surrounding circulating microRNA as potential next generation AML biomarkers. *Leuk Res.* 2015;39(12): 1309-1311.

13. Zhi F, Cao X, Xie X, et al. Identification of circulating microRNAs as potential biomarkers for detecting acute myeloid leukemia. *PLoS One.* 2013; 8(2):e56718.

14. Pandita A, Ramadas P, Poudel A, et al. Differential expression of miRNAs in acute myeloid leukemia quantified by Nextgen sequencing of whole blood samples. *PLoS One.* 2019;14(3):e0213078.

15. Trino S, Lamorte D, Caivano A, et al. MicroRNAs as new biomarkers for diagnosis and prognosis, and as potential therapeutic targets in acute myeloid leukemia. *Int J Mol Sci.* 2018;19(2):E460.